Applied Physics Letters ARTICLE scitation.org/journal/apl

The discrete noise of magnons

Cite as: Appl. Phys. Lett. **114**, 090601 (2019); doi: 10.1063/1.5088651
Submitted: 12 January 2019 · Accepted: 20 January 2019 ·
Published Online: 4 March 2019

View Online Export Citation CrossMark

S. Rumyantsev,[1,2,3,a)] M. Balinskiy,[1,2] F. Kargar,[1,2] A. Khitun,[1,2] and A. A. Balandin[1,2,b)]

AFFILIATIONS

[1]Department of Electrical and Computer Engineering and Phonon Optimized Engineered Materials (POEM) Center, University of California, Riverside, California 92521, USA
[2]Spins and Heat in Nanoscale Electronic Systems (SHINES) Center, University of California, Riverside, California 92521, USA
[3]Ioffe Physical-Technical Institute, St. Petersburg 194021, Russia

[a)]**Present address:** Center for Terahertz Research and Applications, Institute of High-Pressure Physics, Polish Academy of Sciences, Warsaw 01-142, Poland
[b)]**Author to whom correspondence should be addressed:** balandin@ece.ucr.edu. **URL:** https://balandingroup.ucr.edu/

ABSTRACT

We report experimental results, which show that the low-frequency noise of magnonic devices is dominated by the random telegraph signal noise rather than $1/f$ noise—a striking contrast to many electronic devices (f is a frequency). It was also found that the noise level of surface magnons depends strongly on the power level, increasing sharply at the on-set of nonlinear dissipation. The presence of the random telegraph signal noise suggests that the current fluctuations involve random discrete *macro* events caused by an individual macro-scale fluctuator. We anticipate that our results will help in developing the next generation of magnonic devices for information processing and sensing.

Magnonics is a rapidly developing subfield of spintronics, which deals with devices and circuits that utilize spin currents carried by magnons—quanta of spin waves.[1–7] Magnon current, *i.e.*, spin waves, can be used for information processing, sensing, and other applications. A possibility of using the amplitude and phase of magnons for sending signals via *electrical insulators* creates conditions for avoiding Ohmic losses and achieving ultra-low power dissipation.[2–14] Most of the envisioned magnonic logic devices are based on spin wave interference, where the minimum energy per operation is limited by the noise level.[8,11] The sensitivity and selectivity of magnonic sensors are also limited by the low frequency noise.[9,10] However, the fundamental question "do magnons make noise?" has not been answered yet. It is not known how noisy magnonic devices are compared to their electronic counterparts. We still do not know *how different the noise of magnons is from that of electrons*. These intriguing questions are interesting from both fundamental science and practical application points of view. Only recently, theoretical studies on the specific noise types of spin currents started to appear.[15] However, no experimental investigations of the noise of magnons in electrically insulating spin waveguides have been reported. An urgent need to explore this important characteristic for magnonic devices motivates the present study.

The noise in electronic devices, made from metals and semiconductors, can be viewed as various manifestations of the *discreteness* of charges.[16,17] The Johnson–Nyquist thermal noise is associated with the random thermal agitation of electrons, while the shot noise is related to random events of electrons going over a potential barrier.[16,17] The low-frequency $1/f$ noise and generation-recombination (G-R) noise in semiconductors are related to the random process of individual electron caption and emission by the traps associated with defects (f is the frequency).[16–18] With the electron Fermi wavelength $\lambda_F = 2\pi/k_F = 2\pi/(3\pi^2 n)^{1/3} \sim 0.1 - 0.5\,\text{nm}$, the notion of electrons as particles works well for any device size in the context of the noise research (k_F is the Fermi wave vector and n is the charge carrier concentration). Magnons—quanta of spin waves—typically have wavelength, λ_M, in the range from tens of nanometers to hundreds of micrometers and as such retain their essential wave nature in the magnonic devices.[2,5,19] This fundamental difference is expected to affect the random fluctuation processes leading to noise in magnon currents. Understanding the noise characteristics of magnons, particularly at room temperature, is critical for further development of magnon spintronic technology. The low-frequency noise can be up-converted, thus contributing to the phase and amplitude noise near the carrier

frequency, affecting the spectral line width.[16–18] Similar to electronics, the low-frequency noise in magnonics is an ultimate limiting factor of the sensitivity and selectivity of the sensors,[9] communication, and logic devices.[6–8] From the other side, low-frequency noise measurements can serve as an innovative spectroscopy tool, which provides insights into the specifics of the electron or magnon transport.

Both the amplitude and phase noise are important for magnonic device applications. In this study, we focus on the low-frequency *amplitude* noise of magnons, which sets the limits of the performance of the magnonic devices for information processing or sensing.[6–9] The experiments are intentionally conducted on an *archetypal* spin waveguide—main element of all magnonic devices, which utilize pure spin wave currents. The schematic of our waveguide structure is shown in Fig. 1(a). It consists of an electrically insulating yttrium iron garnet (YIG; $Y_3Fe_2(FeO_4)_3$) magnetic waveguide with two micro-strip antennas fabricated directly on top of its surface. One of the antennas is used for magnon excitation by applying RF current. The alternating electric current produces a non-uniform alternating magnetic field around the conducting contour, which, in turn, generates spin waves in the YIG channel under the spin wave resonance conditions. The second antenna is used to measure the inductive voltage produced by the spin wave, *i.e.*, magnon current, propagating in the YIG waveguide. The details of the structure and measurements can be found in the supplementary material.

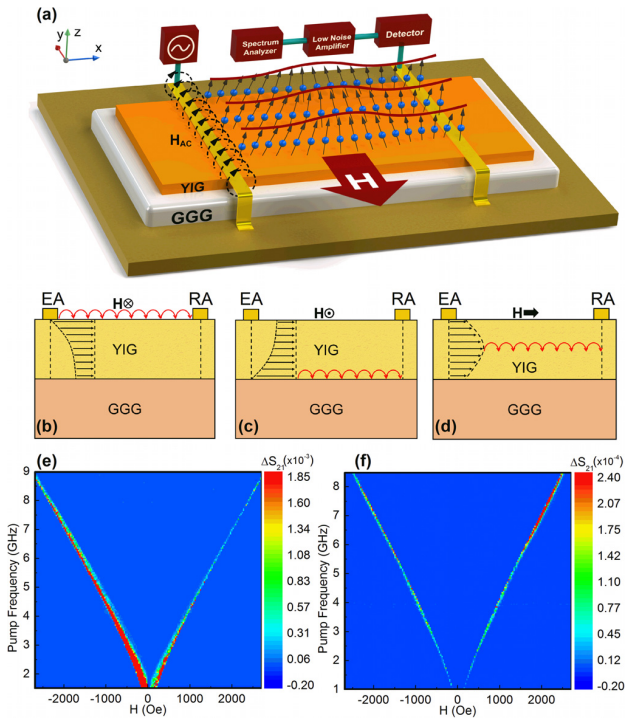

FIG. 1. Spin waveguide structure and types of magnons. (a) Schematic of the device structure showing the spin waveguide, transmitting and receiving antennas, as well as connection of the noise measurement equipment. (b)–(d) Illustration of the propagation of the surface, interface, and volume magnon currents, respectively. (e) The normalized scattering parameter (ΔS_{21}) for the surface (left dispersion branch; negative H) and interface (right dispersion branch; positive H) magnons as a function of the frequency and external DC magnetic field. The dark blue color represents a low output response and the red color a higher output response, corresponding to the propagating magnons. (f) The normalized scattering parameter (ΔS_{21}) for the volume magnons.

We start by confirming the generation and propagation of magnon current through the electrically insulating waveguide. If the bias magnetic field, H, is directed in-plane, along the direction of propagation, the spin waveguide structure supports the backward volume magneto-static spin wave (BVMSW).[20] If H is directed in-plane, orthogonal to the magnon propagation, the structure supports the magneto-static surface spin waves (MSSWs). There are two surfaces for MSSW propagation: the top surface of the YIG waveguide and the interface between the YIG waveguide and the GGG substrate [see Figs. 1(b)–1(d)]. The maximum of the spin wave amplitude is either on the top surface or at the interface depending on the orientation of H. Below, we refer to the three described types of spin waves and corresponding magnons as *surface*, *interface*, *and volume*. The wave vector, k, of the magnon depends on the excitation pump frequency, f_p, and H. Different types of magnons can propagate through the waveguide only at certain combinations of k, f_p, and H. The magnon current reveals itself in the change of the transmission parameter S_{21}[Refs. 3, 5, 21]. Figures 1(e) and 1(f) show the normalized scattering parameters ΔS_{21} ($\Delta S_{21} = S_{21}(H) - S_{21}(H = 0)$) for surface and volume spin waves, *i.e.*, magnon currents as a function of frequency and magnetic field. The normalization procedure allows us to distinguish the spin wave contribution from other effects.[3,9,21] The measured dispersion data were well fitted with the known dispersion laws for BVMSW and MSSW, confirming the types of propagating magnons and allowing for tuning the $f_p - H$ space parameters for the magnon noise studies. These data also confirmed that the signal is not a result of direct electromagnetic coupling between antennas. To minimize the magnon damping, we selected the pump frequency, $f_p = 5.3$ GHz, in the frequency range where the three-magnon dissipation processes are prohibited: $f_p > f_{th}^{3m}$ [Ref. 22]. Here, $f_{th}^{3m} = \gamma 4\pi M_0 \approx 4.9$ GHz is the maximum allowable pump frequency for the three-magnon decay, where $\gamma = 2.8$ MHz/Oe and $4\pi M_0 = 1750$ G is the saturation magnetization of our YIG film.

Propagating in the waveguide, magnon current acquires variations in the amplitude and phase due to the fluctuations of the physical properties of the YIG thin film. To measure these fluctuations, we connected the Schottky diode detector to the receiving antenna [see Fig. 1(a)]. The DC signal from the diode was amplified by a low-noise amplifier and recorded with a spectrum analyzer. As a result, the amplitude noise spectrum of magnons was obtained. The noise was studied separately for the different types of magnons, *i.e.*, spin waves: surface, interface, and volume at a frequency of analysis, f_a, ranging from 1 Hz to ~40 kHz. Figure 2(a) shows attenuation as a function of the input power P_{in}. In the linear, low-power regime, $P_{in} < 5$ dBm, the losses were practically independent of the excitation power and the amplitude noise was below the system sensitivity. In this

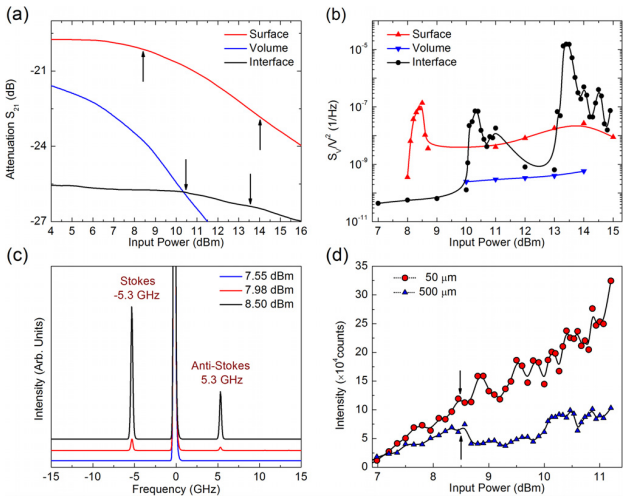

FIG. 2. Propagation and noise of magnons. (a) Attenuation of the surface, volume, and interface magnons as a function of the excitation power at the excitation frequency of $f_p \approx 5.3$ GHz. The arrows indicate the power levels at which the noise attains its maxima. (b) The normalized noise spectral density, S_V/V^2, of the voltage fluctuations at the frequency of the analysis of $f_a = 10$ Hz. Note an abrupt increase in the noise of surface and interface magnons as the input power reaches some threshold level. The noise of volume magnons does not change substantially. (c) Brillouin light scattering spectrum of surface magnons. The magnon peaks are seen at the excitation frequency set by the generator. (d) The intensity of the magnon Stoke peak as a function of the input power for two locations measured from the position of the transmitting antenna. The on-set of strong intensity fluctuations corresponds to the abrupt increase in noise level and on-set of nonlinear dissipation associated with the four-magnon processes.

regime, the noise of magnons expressed in the normalized noise spectral density, S_V/V^2, was below 10^{-11} Hz^{-1} (V is the DC voltage on the Schottky diode). Figure 2(b) presents the noise of the surface, volume, and interface magnons at higher input power at $f_a = 10$ Hz.

The noise of the volume magnons was generally the lowest and revealed only a moderate increase with P_{in}. The increase in P_{in} to some threshold power level, $P_{in} = P_T$, resulted in the abrupt increase in the noise of the interface and surface magnons. The dependence of noise on power for interface magnons reveals two maxima. At the maximum, the noise of the interface magnons is about *two orders of magnitude* higher than that of the surface magnons. The latter was explained by the YIG/GGG interface roughness, resulting in stronger fluctuations of the material parameters that govern magnon current propagation. One should note that even at their peak values, the noise level of magnons was still relatively low. Similar noise levels of 10^{-9} Hz^{-1}–10^{-5} Hz^{-1} are found in conventional transistors and other electronic devices.[23,24]

The arrows in Fig. 2(a) indicate the power levels at which the noise attains its maxima [see Fig. 2(b)]. The noise peak positions correspond to the change of the slope of S_{21} dependence on the power. The change of the slope means the change in the dissipation mechanism, which is driven by the increasing input power. We argue that the amplitude noise peaks are caused by the random switching between two dissipating mechanisms. The situation is similar to the well-known two level systems, where the noise has its maximum close to W(1-W), where W is the probability of the system to be in one of the states.[25] The second mild peak at ~14 dBm for the surface waves in Fig. 2(b) corresponds to another mild change of the slope in S_{21} versus power dependence [Fig. 2(a)]. The dependence of noise and S_{21} for the interface waves is more complicated. However, the correlation between S_{21} and noise peaks can be tracked as well. At this stage, it is impossible to state what specific dissipation mechanisms and transitions between them are seen in Figs. 2(a) and 2(b). The noise peaks likely correspond to the on-set of different types of four-magnon processes, e.g., with different wave-vectors and frequencies. A somewhat similar explanation was proposed for the changes in the power spectrum of the spin-torque oscillators.[26]

Our numerous experiments with several waveguides have shown that P_T of the onset of the high magnon noise of surface waves corresponds to the point of a strong increase in the attenuation, *i.e.*, the offset of the nonlinear dissipation. Given that the pumping frequency $f_p > f_{th}^{3m}$, the dominant nonlinear dissipation mechanism should be related to the four-magnon processes.[22] A rough estimate of the P_{in} value when the four-magnon process for MSSW becomes allowable can be made as[27] $P_{th}^{4m} \approx m_{th}^2 V_g w d$, where V_g is the magnon group velocity, w is the film width, d is the film thickness, and m_{th} is the threshold amplitude of variable magnetization defined by the film magnetic properties. Using measured $V_g = 1.25 \times 10^7$ cm/s, geometry, and m_{th} from the literature,[22,27] we estimate $P_{th}^{4m} \approx 0.24$ mW, which is below the typical pumping level in our experiments. The latter indicates that for the selected f_p and $P_{in} \geq P_{th}^{4m}$, the four-magnon processes are allowed in our system.

In the four-magnon scattering, two magnons of frequency f_p annihilate and create a pair of quickly dissipating magnons of close frequencies and counter directed k-vectors.[11,22] At some density of initial magnons, these processes become avalanche-like, leading to a sharp decay of the initial magnon current. The first peaks in the noise spectral density of the surface magnon currents appear at the onset of the avalanche-like four-magnon processes (~8 dBm) when the system fluctuates between the linear and non-linear regimes [Fig. 2(b)], and the factor W(1-W) is at its maximum. A further increase in P_{in} leads to a reduction in the noise when the system stabilizes to a certain type of four-magnon process, *i.e.*, W(1-W) factor decreases, followed by the second peaks, which likely correspond to the on-set of other types of four-magnon processes, e.g., with different wave-vectors and frequencies.[22] It is interesting to note that the noise signatures of the four-magnon processes–abrupt few-orders-of-magnitude peaks [Fig. 2(b)]–are much more clear than the corresponding gradual changes in the amplitude attenuation slopes [Fig. 2(a)]. Until now, most of the nonlinear magnon scattering was studied using the time-resolved magneto-optical Kerr effect[28] or Brillouin spectroscopy.[29] The demonstrated ability to monitor nonlinear magnon damping phenomena via noise spectroscopy provides a powerful tool for studying multi-magnon processes.

To provide independent confirmation of the correlation of the magnon current noise with the onset of strong multi-magnon

processes, we conducted *in-situ* Brillouin–Mandelstam spectroscopy (BMS) of the propagating magnons.[30,31] The details of the BMS experiment can be found in the supplementary material and our previous reports on other material systems.[32–35] In these experiments, we focused laser light on a YIG channel and varied the input RF power. Figure 2(c) shows the representative BMS spectra with clear Stokes and anti-Stokes signatures of the surface magnons at the pump frequency. At a low power level, $P < 7$ dBm, the intensity of the Stokes peak is close to the sensitivity limit of our instrument. With the power increase, the intensity of the peaks increases approximately linear with the power [see Fig. 2(d)]. At the power level $P > 8.5$ dBm, the dependence becomes strongly non-monotonic and unstable. One can see a decrease in the intensity for the 500-μm beam location and the intensity oscillations for the 50-μm beam location. The noise level increases sharply at the same power level [Fig. 2(b)], indicating the on-set of nonlinear dissipation.

The magnon noise spectrum as a function of frequency revealed another unusual feature. The spectra of the amplitude fluctuations had the shape of the clear Lorentzian, $S_V \sim 1/(1+f^2/f_c^2)$ with the characteristic corner frequency $f_c < 100-1000$ Hz [see Fig. 3(a)]. This is in striking contrast to macroscopic electronic devices where the low-frequency noise is usually dominated by either $1/f$ noise or its superposition with G-R noise.[17,18,36] In the time domain, the magnon noise revealed itself as a random telegraph signal (RTS) noise, appearing as a series of pulses of the fixed amplitude and random pulse width and time intervals between the pulses. The representative recordings of RTS noise of magnons are shown in Fig. 3(b). Interestingly, very small changes in P_{in} resulted in significant changes in the magnon noise characteristics. The level and shape of the noise spectra as well as the shape of the RTS traces changed strongly with the power input. The RTS noise is well known in semiconductor devices.[36] It appears when a single fluctuator makes a dominant contribution to noise. For example, in a field-effect transistor with a very small gate area, RTS is due to the capture and emission of an electron by a *single* trap.[37] The RTS noise always has the form of the Lorentzian [Fig. 3(a)]. However, the Lorentzian type of spectra does not always represent the RTS noise. Our observation of RTS noise in the large magnon waveguides suggests that in the nonlinear dissipation regime, individual *discrete* macro events contribute to both the noise and magnon dissipation processes. We found this kind of RTS noise in *all* studied magnonic devices, which suggests that this is a specific feature of nonlinear dissipation process of magnons. At high frequencies, the noise decreases as $1/f^2$ and falls below the background noise level. A possible mechanism of the avalanche-like process, leading to RTS noise, can be the so-called self-organized criticality, which was introduced to explain the fractals and avalanches generated spontaneously in dissipative systems.[38] It has been demonstrated that this mechanism can be applied to systems with different types of spectra and avalanches, e.g., RTS noise.[39,40] Recent theoretical work on the magnonic noise[41] suggests the existence of regimes where noise spectral density has RTS-like dependence, in line with our experimental observations.

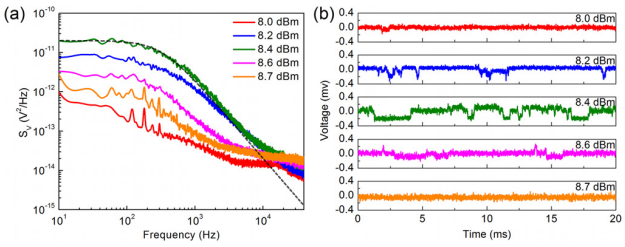

FIG. 3. Magnon noise and discrete fluctuators. (a) Noise spectra for five slightly different input power levels, corresponding to the first noise maxima for surface magnons in Fig. 1(b). The low-frequency noise has pronounced Lorentzian characteristics, which is in striking contrast to $1/f$ noise in macroscopic electronic devices. (b) The random telegraph signal noise of magnons shown in the time domain for the same input power levels. The data are presented for $f_0 \approx 5.3$ GHz. The well-defined RTS noise is an indication that a single discrete fluctuator makes a dominant contribution to noise.

In the majority of cases, in electronic devices, the low-frequency noise scales inversely proportional to the number of the fluctuators in a device, i.e., inversely proportional to its volume or area. The situation is different when RTS is the main noise type. If the noise is dominated by a single discrete fluctuator, the reduction of the device area does not necessarily change the number of fluctuators until the device area is of the order of the dimension of the fluctuator itself. The size of the fluctuator can be roughly estimated if we assume that this fluctuator blocks the spin wave completely. Following the analogy with the charge density waves,[42] we can write that $\delta A/A = \delta V/V$, where δA is the area of the fluctuator, $A = w \times L_D$ is the total active area of the device, w is the width of the YIG waveguide, and L_D is the characteristic length, related to the wave attenuation, and $\delta V/V \approx 10^{-2}$ is the relative amplitude of the RTS noise. This estimate yields the area $\approx 10^4$ μm^2. In comparison with semiconductor devices, this is a very large area. However, it is still orders of magnitude smaller than the total area of the studied YIG waveguide. The latter means that the A^{-1} scaling may not apply for magnons, and smaller magnon devices do not automatically become noisier. Additional investigations are needed to verify this projection when the magnon device technology matures sufficiently to yield a wide range of device sizes. The wavelength of spin waves in our experiments can be estimated as $\lambda_M = 2\pi L/\Psi_T$, where Ψ_T is the total phase difference accumulated over the propagation distance between antennas, L. With Ψ_T directly measured by VNA, we obtained $\lambda_M \approx 390$ μm, which confirms the large spatial extent of magnons in our experiments. The large wavelength and spatial extent of magnons create conditions for the single fluctuator mechanism in macroscopic devices at RT. This is in contrast to electronic devices, where the single fluctuator mechanism becomes pronounced in sub-micron dimensions and cryogenic temperatures or nanometer scale dimensions and temperatures up to RT. Owing to their small Fermi wavelength, electrons mostly behave as particles in the noise context.

The concentration of magnons in our devices, n_M, can be roughly estimated *as* $n_M = m^2/(2M_0\gamma h)$, where m is the variable magnetization, M_0 is the saturation magnetization, $\gamma = 2.8$ MHz/Oe, and h is Planck's constant.[22] Taking $M_0 = 139$ Oe for YIG, we obtain $n_M \approx 2 \times 10^{17}$ cm^{-3}. For a given

magnon concentration, the large amplitude of the RTS signal, $\delta V/V \approx 10^{-2}$, indicates that a large number of magnons disappear during a single step of the RTS signal. The latter suggests an unusual RTS noise of magnons as compared to electrons in electronic devices. For example, in downscaled metal-oxide-semiconductor field-effect transistors, a single RTS step can correspond to just *one* electron captured by the trap.[17,36,37] Therefore, the RTS-like signal found in magnonic devices is different from classical RTS noise in semiconductor devices and has certain inherent discreteness revealed via individual fluctuation events of spatially large fluctuators with unusually high amplitude.

In conclusion, we investigated the noise of magnon currents in electrically insulating spin waveguides. It was discovered that the low-frequency amplitude noise of magnons is dominated by RTS noise, unlike the noise of electrons in conventional devices, which is mostly dominated by $1/f$-like noise. Our findings suggest that the noise of wave-like magnons, characterized by their large spatial extent, and the high number of magnons participating in each RTS step reveal an unusual *discrete* nature. It is also rather muted, or *discreet*, at the lower power levels. We have established that the volume magnons produced much less noise than surface and interface magnons. The noise of surface and interface magnons increases sharply at the on-set of nonlinear processes. It was also demonstrated that noise spectroscopy can serve as a valuable tool for investigating non-linear magnon dissipation.

See supplementary material for the details of the device structure, noise measurement, excitation and detection of spin waves, and Brillouin-Mandelstam spectroscopy of spin waves.

The work at UC Riverside was supported as part of the Spins and Heat in Nanoscale Electronic Systems (SHINES), an Energy Frontier Research Center funded by the U.S. Department of Energy, Office of Science, Basic Energy Sciences (BES) under Award No. SC0012670. The authors are indebted to H. Chiang for performing metal deposition, J. S. Lewis and Z. Barani for assistance with BMS measurements, and E. Hernandez for his help with the device schematics.

REFERENCES

[1]S. A. Wolf, D. D. Awschalom, R. A. Buhrman, J. M. Daughton, S. Von Molnár, M. L. Roukes, A. Y. Chtchelkanova, and D. M. Treger, Science **294**, 1488 (2001).
[2]A. V. Chumak, V. I. Vasyuchka, A. A. Serga, and B. Hillebrands, Nat. Phys. **11**, 453 (2015).
[3]S. A. Nikitov, D. V. Kalyabin, I. V. Lisenkov, A. Slavin, Y. N. Barabanenkov, S. A. Osokin, A. V. Sadovnikov, E. N. Beginin, M. A. Morozova, Y. A. Filimonov, Y. V. Khivintsev, S. L. Vysotsky, V. K. Sakharov, and E. S. Pavlov, Phys.-Usp. **58**, 1002 (2015).
[4]G. Csaba, Á. Papp, and W. Porod, Phys. Lett. A **381**, 1471 (2017).
[5]S. O. Demokritov and A. N. Slavin, *Magnonics: From Fundamentals to Applications (Topics in Applied Physics)* (Springer Science & Business Media, 2012).
[6]S. Dutta, D. E. Nikonov, S. Manipatruni, I. A. Young, and A. Naeemi, Sci. Rep. **7**, 1915 (2017).
[7]S. Neusser and D. Grundler, Adv. Mater. **21**, 2927 (2009).
[8]A. Khitun, M. Bao, and K. L. Wang, J. Phys. D. Appl. Phys. **43**, 264005 (2010).
[9]M. Balynsky, D. Gutierrez, H. Chiang, A. Kozhevnikov, G. Dudko, Y. Filimonov, A. A. Balandin, and A. Khitun, Sci. Rep. **7**, 11539 (2017).
[10]P. Talbot, A. Fessant, and J. Gieraltowski, Procedia Eng. **120**, 1241–1244 (2015).
[11]A. V. Chumak, A. A. Serga, and B. Hillebrands, Nat. Commun. **5**, 4700 (2014).
[12]L. J. Cornelissen, J. Liu, R. A. Duine, J. B. Youssef, and B. J. van Wees, Nat. Phys. **11**, 1022 (2015).
[13]A. Haldar, C. Tian, and A. O. Adeyeye, Sci. Adv. **3**, e1700638 (2017).
[14]H. Nakayama, T. Yamamoto, H. An, K. Tsuda, Y. Einaga, and K. Ando, Sci. Adv. **4**, eaar3899 (2018).
[15]A. Kamra and W. Belzig, Phys. Rev. B **94**, 014419 (2016).
[16]A. der Ziel, *Noise* (Prentice-Hall, 1954).
[17]S. Kogan, *Electronic Noise and Fluctuations in Solids* (Cambridge University Press, Cambridge, 2008).
[18]P. Dutta and P. M. Horn, Rev. Mod. Phys. **53**, 497 (1981).
[19]C. Liu, J. Chen, T. Liu, F. Heimbach, H. Yu, Y. Xiao, J. Hu, M. Liu, H. Chang, T. Stueckler, S. Tu, Y. Zhang, Y. Zhang, P. Gao, Z. Liao, D. Yu, K. Xia, N. Lei, W. Zhao, and M. Wu, Nat. Commun. **9**, 738 (2018).
[20]R. W. Damon and J. R. Eshbach, J. Phys. Chem. Solids **19**, 308 (1961).
[21]O. Rousseau, B. Rana, R. Anami, M. Yamada, K. Miura, S. Ogawa, and Y. Otani, Sci. Rep. **5**, 9873 (2015).
[22]A. G. Gurevich and G. A. Melkov, *Magnetization Oscillations and Waves* (CRC press, New York, 1996).
[23]Z. Celik-Butler and T. Y. Hsiang, Solid State Electron. **30**, 419 (1987).
[24]A. Balandin, S. V. Morozov, S. Cai, R. Li, K. L. Wang, G. Wijeratne, and C. R. Viswanathan, IEEE Trans. Microwave Theory Tech. **47**, 1413 (1999).
[25]Y. M. Galperin, V. G. Karpov, and V. I. Kozub, Adv. Phys. **38**, 669 (1989).
[26]J. Von Kim, Q. Mistral, C. Chappert, V. S. Tiberkevich, and A. N. Slavin, Phys. Rev. Lett. **100**, 167201 (2008).
[27]G. T. Kazakov, A. V. Kozhevnikov, and Y. A. Filimonov, Phys. Solid State **39**, 288 (1997).
[28]J. Fassbender, Spin Dyn. Confin. Magn. Struct. II **87**, 59 (2003).
[29]O. Büttner, M. Bauer, S. O. Demokritov, B. Hillebrands, Y. S. Kivshar, V. Grimalsky, Y. Rapoport, M. P. Kostylev, B. A. Kalinikos, and A. N. Slavin, J. Appl. Phys. **87**, 5088 (2000).
[30]S. O. Demokritov, V. E. Demidov, O. Dzyapko, G. A. Melkov, A. A. Serga, B. Hillebrands, and A. N. Slavin, Nature **443**, 430 (2006).
[31]M. Balinskiy, F. Kargar, H. Chiang, A. A. Balandin, and A. G. Khitun, AIP Adv. **8**, 056017 (2018).
[32]F. Kargar, E. H. Penilla, E. Aytan, J. S. Lewis, J. E. Garay, and A. A. Balandin, Appl. Phys. Lett. **112**, 191902 (2018).
[33]M. M. Lacerda, F. Kargar, E. Aytan, R. Samnakay, B. Debnath, J. X. Li, A. Khitun, R. K. Lake, J. Shi, and A. A. Balandin, Appl. Phys. Lett. **110**, 202406 (2017).
[34]F. Kargar, B. Debnath, J.-P. Kakko, A. Saÿnätjoki, H. Lipsanen, D. L. Nika, R. K. Lake, and A. A. Balandin, Nat. Commun. **7**, 13400 (2016).
[35]F. Kargar, S. Ramirez, B. Debnath, H. Malekpour, R. K. Lake, and A. A. Balandin, Appl. Phys. Lett. **107**, 171904 (2015).
[36]V. Mitin, L. Reggiani, and L. Varani, in *Noise and Fluctuations control in Electronic Devices*, edited by A. A. Balandin (American Scientific Publishers, Los Angeles, 2002), pp. 11–29.
[37]M. J. Kirton and M. J. Uren, Adv. Phys. **38**, 367 (1989).
[38]P. Bak, C. Tang, and K. Wiesenfeld, Phys. Rev. Lett. **59**, 381 (1987).
[39]J. Kertesz and L. B. Kiss, J. Phys. A: Math. Gen. **23**, L433 (1990).
[40]S. S. Manna, L. B. Kiss, and J. Kertész, J. Stat. Phys. **61**, 923 (1990).
[41]K. Nakata, Y. Ohnuma, and M. Matsuo, Phys. Rev. B **98**, 094430 (2018).
[42]I. Bloom, A. C. Marley, and M. B. Weissman, Phys. Rev. Lett. **71**, 4385 (1993).